A Novel Approach on Dehazing Volcanic Crater Lake Hazy Scene Videos Based on Color Attenuation Prior

by Agus Prayitno

Submission date: 22-Sep-2021 10:24PM (UTC-0500)
Submission ID: 1655277237
File name: ater_Lake_Hazy_Scene_Videos_Based_on_Color_Attenuation_Prior.pdf (1.02M)
Word count: 10075
Character count: 50233

Praise Worthy Prize

International Review on Computers and Software (I.RE.CO.S.), Vol. 12, N. 1
ISSN 1828-6003 January 2017

A Novel Approach on Dehazing Volcanic Crater Lake Hazy Scene Videos Based on Color Attenuation Prior

Oddy Virgantara Putra[1,2], Budi Prianto[3], Agus Prayitno[1,4], Esther Irawati Setiawan[1,5], Eko Mulyanto Yuniarno[1], Mauridhi Hery Purnomo[1]

Abstract – *A crater lake of Mt. Kelud active volcano formed after the eruption on February, 2014. Real time surveillance has been conducted for 24 hours using a CCTV camera on the top of the summit. The primary purpose of this observation is monitoring the volcanic activity, such as degassing and discoloration of crater lake water. These phenomenons became the symptoms of the volcanic activity. The weather condition is continuously changes between clear, cloudy, and hazy. Obviously, camera vision is obscured or even blocked by haze. Another problem is that airlight source is hard to estimate because the lake color tends to be brighter in clear conditions. In this paper, a dehazing technique is proposed based on color attenuation prior and contrast enhancement. In contrast enhancement, the transmission map was enhanced using adaptive gamma correction. Our data were analyzed using referenceless fog density estimation (FADE). Our experimental results give the best result when it comes to fog density (by 1.60912 density) compared to previous algorithms.*

Keywords: *Active Volcano, Adaptive Gamma Correction, Airlight, Color Attenuation Prior, Degassing, Dehazing, Eruption*

Nomenclature

γ	Adaptive Gamma Correction
a	Atmospheric light source
v,s	Brightness and saturation respectively
$\lambda_1,\lambda_2,\lambda_3$	Coefficient in color attenuation model
d	Depth of the scene within video frames
e	Euler's number or exponential
h	Haze concentration
I	Input hazy video frames
z,V_{maks}	Intensity and Intensity maximum from grayworld
P,**r**,**f**	Matrix, Vectors
$tmap(m)$	Medium transmission
$p(m)$	Patch centered at m size 15×15 pixel
m	Pixel coordinate within frames
J	Restored scene radiance
β	Scattering coefficient at the atmosphere

I. Introduction

Mt. Kelud is one of Indonesia's active stratovolcanoes that is exactly located adjacent to the three big cities in East Java, Kediri, Blitar, and Malang. Mt. Kelud also has an attractive lake. This lake has the most wonderful view in the southeastern region of the Kediri district and is located 1.7 kilometers above sea level.

The lake stands in the middle of the three peaks. Many eruptions happened, almost every 30 years according to historical data about the eruption [1]. An explosion in 2007 created a "Lava Dome", which covered the whole lake. The explosion started with the discoloration of the lake water and a degassing process on the edge of the lake. Afterwards, the lake completely disappeared.

After 7 years, one of the most massive eruptions happened on February 14th, 2014. It begun with gas and smog ascending to the sky [2], [3]. Along with them, a thunder started rumbling above the mountain. Even people living far away from the incident heard the sound of the thunder. It was dark, with a sand rain covering rooftops. A week later, the ashes covered the whole Kediri city and the area located towards southwest, west, and north. Even Bandung city, which is 500 kilometers away from Kediri, was affected. Nearly a month after the eruption the crater lake reappeared.

Learning from the signs [4]–[6] prior to the eruption, the government from Indonesia prioritized this into a national development plan for disaster mitigation. They delegated the Mt. Kelud's observers to start conducting surveillance using two CCTV cameras in addition to the seismograph. The cameras are planted on the top two of the three summits of the mountain. They are facing down directly to the lake and covering the whole lake. Sulfur Dioxide is triggered due to the increase of volcanic activities which cause degassing [7]–[12]. The gas flux [8], [12], [13] began spreading and rotating around the

https://doi.org/10.15866/irecos.v12i1.11735

lake. Because of this phenomenon, the volcanic observers could not monitor conditions of the lake such as lake color, water elevation, and the spread of gas. Numerous research activities have been conducted in Mt. Kelud, such as those on the seismic, water, and gas content. However, in terms of computer vision, especially analysis and processing the hazy scene video had not been executed before.

Naturally, in certain conditions, it is hard to estimate the color of the lake. The scene color is strongly influenced by the luminance of the sunlight which is reflected by the lake and scattered by the thick haze. The heavy fog causes the scene color to become green. The scene tends to be yellow when the weather is clear. The authors focused on restoring the color in hazy condition. Due to the influence of scene color, it was a challenging tas

In this paper, an enhanced dehazing method is proposed to restore the color and visibility of the video captured by the CCTV. Using color attenuation prior proposed in [14] the scene depth of crater lake was estimated and adaptive gamma correction (AdaptGC) was used to enhanc the dehazing result. By incorporating [14]–[17], a dehazing technique was used with the following steps: input hazy scene, the dark channel taken as the basis for extracting a source of light, depth estimation using linear equation, transmission map estimation and enhancement using AdaptGC, scene restorat and guided image filtering.

The rest of the paper is organized as follows: Section II reviews the previous works related to this method. Section III elaborates the proposed work. Section IV explains experiments and the results. The results were evaluated using the referenceless fog-aware density estimation (FADE) [18]. Section V presents the conclusion of the research.

II. Related Works

In recent years, a number of researches have been developed on dehazing. Improvements are achieved due to multidiciplinary assumptions and approaches. A haze removal technique based on Independent Component Analysis (ICA) was proposed by [19] (Fattal *et al*). The author assumed that there is a local uncorrelation between surface shading and the transmission medium. The hazy image model has been refined by Fattal in his work by adding the albedo constant vector **R** and scalar l. Those two variables replaced the definition of haze-free image. This albedo came from an ambiguity in three equations for every pixel within inp image. Fattal's method estimates the transmission by using Gauss-Markov random field. This method also estimates the proportion he white light reflected by a surface or an object. His method is able to refine the transmission by estimating the albedo of the scene. This smoothing process took long enough for one frame to process. The shortcoming for this method is its inability to handle denser haze images.

Assuming that on the local contrast is higher in clear scenes than in obscured scenes, a Markov Random Field (MRF)-based method has been proposed for dehazing by maximizing local contrast [20]. One of the problems of visibility in bad weather is the absence of atmospheric light (atm light). This is due to the overcast from the sky, which makes the atm light remain globally constant. The task is more focused on estimating the chromaticity of light instead of estimating atm light. The process is named normalizing object chromaticity. Tan mentioned that there are some clues that must be satisfied in case of hazing problems. First, the output image clear scene must have higher contrast than the input hazy image. Second, the high variance values of atm light depend on the depth of the image. Therefore, at a certain patch, atm light tends to be the same at the same depth. Third, bad weather usually disrupts hazy input images because they are outdoor images. Thus, the recovered scene must address the features of a clear scene. This method results in an impressive clear image which has less contrast but is still prone to oversaturation. This is due to high distinctive contrast level between adjacent patches and might contain block-like window artifacts on short distance. The artifacts make the result look unnatural.

If we observe an image, in most of patc from natural scene except sky region, at least there is one color channel in the RGB color space which has low intensity, and almost down to zero. For example, consider a scene like tree leaves, blue flowers, red roofs, etc, in RGB color space, the tree leaves have the highest green channel compared to the remaining channels. For blue flowers, the blue channel tends to be the highest color channel. This was called DCP and introduced by He [15]. By using this assumption, the patches with a dark area are clearly considered not as the source of light. The result of DCP can handle denser haze. However, this method failed when it comes to the region with bright color such as the sky, lake color reflecting the sunlight, and white objects. In addition to failing in atm light estimation, the DCP may contain halo effects on the edge. The other problem of this method is that transmission map result contains a halo effect around the edge of the object. The restored image became block-like patch. To overcome this problem, the block is smoothed using a soft matting algorithm to improve the output quality, even if the filtering process is long. In the following year, He *et al* [16] proposed a filter by using image as a guide to improve the process time of matt filtering. The DCP method may result in oversaturation if there is any object brighter than atm light.

A new method in transmission restorat n was introduced by Meng *et al* [21]. This method is based on L1-norm for weighting contextual regularization. This method also inherited from DCP for restoring the scene radiance which limit the boundary constraint. Meng introduced a new geometry for the hazy image model. This model is in radiance cube with two additions which are C_0 and C_1 as lower and upper boundary constraint limit respectively. The weighting came from the

assumption that, in local patch, the neighboring pixels share a similar depth. Meng claimed that, in his case, the L1-norm is more robust than the L2-norm, but may fail on minimizing halo effect.

Zhu *et al* [14] proposed the depth model based on the observation of linearly correlated brightness and saturation. Assumming that in natural hazy scenes the distance between camera and the scene is far, the scene depth is limited to a certain threshold. To put it simply, the task of Zhu's method depends on recovering the depth map. They observed a natural scene where near objects and far objects were separated in the hazy scene. This observation resulted that in near object, where the scene is uninfluenced by haze, the saturation statistically increased. When in moderate distance, where the haze is slightly influencing, the saturation gets lower when brightness starts to increase. And for far objects, where the haze almost completely took over the scene, the saturation statistically decreased and brightness drastically increased. The most interesting part of this observation is that saturation and brightness are correlated to the distance of the scene. The denser the haze, the larger the difference between saturation and brightness. The term color attenuation prior (CAP) came from this positive statistic correlation, where scene depth, haze concentration and brightness minus by saturation are related. In the linear depth model, there are some coefficients that must be optimized using the supervised method. The CAP is pretty fast and able to preserve the edge color compared to the other method. The shortcoming of this method is that when an object in scene is near, it may get darker. Popular recent works are based on the DCP, which states that clear images locally have a low intensity in one or two color channels. Some adaptive researches have been used in [15], [22]. And the most recent research is based on machine learning [14], [23]. The key for dehazing is to estimate the transmission map [14], [23].

Based on the Convolutional Neural Network (CNN), [23] proposed an end-to-end system for estimating the medium of transmission called DehazeNet. The DehazeNet used a non-linear activation function for its cascaded convolution. This method extracts several features relevant to haze such as dark channels, hue disparity, and color attenuation. Cai *et al* evaluated the results of his DehazeNet using component robustness evaluation (CRE) and airlight robustness evaluation (ARE). The CAP achieves the best result for thinner haze density when the scattering coefficient β is equal to 0.75. The performance gradually decreased when the haze is thicker. Recently, a dehazing method was proposed by Galdran *et al* [24]. This method was called Fusion-based Variational Image Dehazing (FVID). Galdran's approach used three stages. First, the variance of image-dehazing energy (EVID) is minimized. But, this step is prone to overcontrast the adjacent area. The next stage is storing the original image with its related dehazed output. Then, both steps are fused to get better results.

In the future, not only the haze removal process is crucial in terms of visibility restoration but also color restoration and video dehazing. A video based algorithm for dehazing was proposed by Kim *et al* [25]. Generally, atm light is assumed to be the brightness color [14], [15], [26]. Zhu *et al* estimated the atm light by picking the top 0.1 % in the dark channel domain as well as He's. Zeng and Dai picked the maximum intensity from each color RGB channel in color image. In Kim *et al* method, atm light was estimated by quad-tree subdivision. The image is divided into four rectangular-shaped blocks. Then, each image is divided again recursively until it reaches a certain threshold. This method achieves the right atm light on the sky region. However, Kim's method for estimating the atm light may fail when under minimum possession of sky region. In terms of transmission map estimation, Kim used an optimized method by minimizing the mean-squared error (MSE) contrast cost function and information loss cost function.

An underexposed video enhancement based on the perception-driven progressive fusion was proposed by [27] Zhang *et al*. The noise and visual artifact in the video can be reduced by preserving the texture. Underwater image enhancement is interesting to take into account, since the information of the red channel and green channel is loss for deeper water [28]–[30].

In case of color restoration, a polynomial equation based method was proposed by Pujiono *et al* [21] for coral reef underwater images. This polynomial is based on the constancy of red, green, and blue colors in water. There are two steps in this method. First, determining the underwater color constancy function. Second, from previous function, the coefficients are estimated by using ordinary least squares. Pujiono's result is better than CLAHE in Peak Signal-to-Noise Ratio (PNSR) and is able to restore the image in clear sea water conditions. However, this method may fail when water is overcast.

To overcome the problem in heterogenous underwater conditions, a two-way method in output enhancement for underwater image color restoration was proposed by Li *et al* [29]. The first way is to restore the natural and genuine color appearance. The other way is to improve the brightness and contrast by using a prior from the histogram distribution. This method was based on observation from the distribution of images from scene in the outdoor. In estimating atm light for underwater images, one cannot simply use the global outdoor assumption as mentioned in [14], [15], [21], [25]. An object might be brighter than the atm light itself. Li incorporated the atm light extraction in underwater images from [25] as a quad-tree subdivison hierarchical search, DCP [15] as effect removal for suspended particles, and determining the global atm light from the direction of light.

Since blue has has a shortest wavelength [28], [29] compared to green and red, it is certain that the direction of atm light comes from a region which contains the brightest red pixels. For loss information reduction, the transmission map in the red channel is optimized.

This is due to the fact that the red channel is the most representative for underwater images whereas the remaining two channels are representative for outdoor images. This method also gives results with reduced artifacts.

In previous research, [31] has proposed method for dehazing based on DCP. But, the recovered image color is still dominated by global luminance.

Gupta *et al* [30] proposed an efficient and adaptive contrast enhancement method for images using the gamma correction and probabilistic distribution of chromaticity pixels. This method contains two steps. The first step is enhancing the brightness and contrast by modifiying luminance pixel distribution. The second step used a color restoration framework to maintain the color tone. The result of the method is able to preserve color information.

The next adaptive color enhancement is from [17]. Huang proposed an AdaptGC based on a cumulative probability density function (CDF). This method cumulatively sums up the probability density function (PDF) of the grayworld image histogram. The result is capable of restoring the low brightness image. The shortcoming from this method is less effectiveness on hazy scene images.

Some methods adapt the use of contrast limited adaptive histogram equalization (CLAHE) [32], [33]. A low light scene may result high noise and distortion [32]. The captured images in such a dark scene may contain large size of dark block pixel, low visibility, and low image quality. Jung *et al* algorithm converts the RGB color into YUV color space. By enhancing the low light image with a low-pass subband, this method yields a clearer image. In biomedical imaging, a bioorthogonal spline wavelet based on CLAHE is used in [33] for cephalograms. A standard histogram equalization may leads to overcontrast. This overcontrast was called spikes. The spikes appear when the pixel which have similar intensity are present into homogeneous blocks. These spikes generate more noises and change the distribution of pixel intensity of images. To overcome this problem, enhanced version of CLAHE was proposed.

III. Proposed Method

Obscured scene on top of the mountain happened due to solfatara [1], [11], [12]. This chemical reaction releases many kinds of gases, such as: SO_2, H_2O, carbon monoxide (CO), carbon dioxide (CO_2), H_2S, N_2. Moreover, if certain gas interact with rocks, it will induce other compounds.

Mostly, the scene radiance of the lake in the video is affected by its surroundings. This luminance comes from the vegetation around the lake and from the lake color itself. Airlight plays a huge role in dehazing, especially the dark channel prior (DCP). In our case, the camera view does not cover the sky area, as seen in Fig. 2.

From time to time, the scene color keeps changing. In the thick cloud condition, it becomes dark green. And in a clear condition, it becomes light brown. Based on these conditions, the authors mainly focused on restoring the lake color in hazy conditions.

In this part, the proposed method was elaborated. The authors focused on dehazing process by selecting fast dehazing algorithm and enhancing its contrast yields more natural scene. Fig. 1 shows the block diagram of the proposed algorithm. For the first step, the video was extracted per frame.

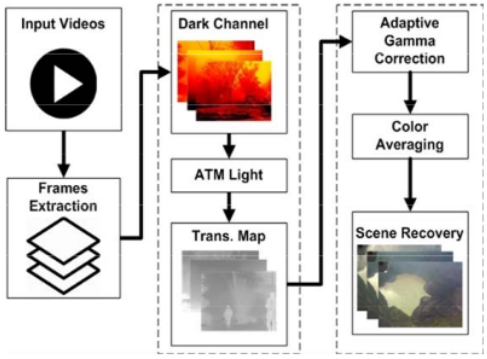

Fig. 1. Proposed method. We incorporated dehazing method from Zhu *et al* for depth estimation, adaptive gamma correction from Zhang *et al*, Huang *et al* for color averaging (CA)

Second, the dark channel of each frame was taken for input hazy scenes. Then, the atm light in dark channel images was estimated. The next step was to determine the depth of input hazy images using the CAP model. After the depth has been determined, the medium transmission map can be estimated.

Prior to the last step for scene restoration procedure, we first need to enhance color using AdaptGC and color averaging.

The lake is located at 7° 56' 15.6156" S and 112° 18' 15.3072" E (see Fig. 3) and monitored in real-time using CCTV camera model Axis Q1755-E Network Camera, with resolution 1280 × 720 and 10× optical and 12x digital.

Fig. 2 CCTV field of view (FOV) above the lake

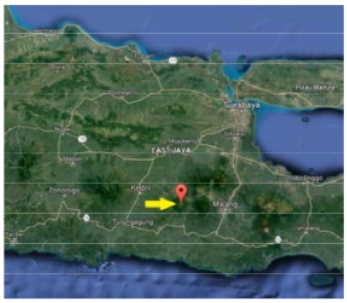

Fig. 3. Location of Mt. Kelud, East Java Province, Indonesia

III.1. Hazy Image Modelling

According to [34], [35], the image model on hazy weather can be modelled as:

$$\mathbf{I}_c(m) = \mathbf{J}_c(m)\,tmap(m) + \mathbf{a}\left(1 - tmap(m)\right) \quad (1)$$

where m is the coordinate position of pixels within the image, c is the RGB color channel, $\mathbf{I}$ is the input hazy scene, $\mathbf{J}$ is radiance of scene, $tmap$ is the transmission medium map, $\mathbf{a}$ is the light of atmosphere.

When it comes to a homogeneous atmosphere condition, the transmission medium rate $tmap$ can be defined as:

$$tmap(m) = e^{-\beta d(m)} \quad (2)$$

where β represents the scattering coefficient in the atmosphere. It is important to consider that $tmap$ depends on $d(m)$, since the coefficient β is ignored due to the homogeneity of the atmosphere [14], [22]. And $d(m)$ is the depth of image. The purpose of this equation is simply to extract the $\mathbf{J}$ in Eq. (1) from $\mathbf{I}$. In spite of the fact that $tmap$ remains constant in the local patches. From Eq (1) and Eq (2), we know that:

$$0 \le tmap(m) \le 1 \quad (3)$$

As additional information, the attenuation model is described in left side in Eq (1) by the term $\mathbf{J}_c(m)\,tmap(m)$. It means that the clear scene is directly transmitted through the medium without any disruption. However, in natural hazy scenes, the next term is called air-light, which is represented by $\mathbf{a}\left(1 - tmap(m)\right)$ from the right side in Eq (1). This means that additional element mean is fused [15], [20], [26], [36].

III.2. Color Attenuation Prior

Since DCP is prone to oversaturation for brighter objects and gets darker when it fails on achieving low atm light, Zhu [14] assumed that d is large enough for the given certain threshold. Estimating $\mathbf{a}$ is probably most suitable than calculating $\mathbf{a}$. Thus, when d reaches its threshold it means that:

$$\mathbf{I}_c(m) = \mathbf{a} \quad (4)$$

In hazy scene, an object far from the observers naturally lies at great distance. Obviously, the distant object has large depth. Consider that the depth is limited to certain threshold d_t. From this condition, the remaining task is the depth estimation.

Restoring the view for video processing is a challenging task. This is due to the minimum information and the need of brief process for each frame. According to the computer vision principle, human eyes can clearly distinguish haze and natural objects. Inspired by [14], it was found that brightness and saturation of natural scenes are linearly correlated. As illustrated in Figs. 4, a near haze-free region has high saturation and low brightness (see Fig. 4(d)). Along with the high density of the haze, the saturation also decrease. The lower the value of saturation the nearer the object to white. For middle range (see Fig. 4(c)), it was found that saturation and brightness are nearly equal. And for more distant objects (see Fig. 4(b)), saturation decreases and brightness increases. This is mainly caused by the high influence of haze [20], [34], [35]. A naturally obscure scene, which is affected by haze, happens at a distant area. Cumulative haze gets thicker along with object range [15]. This is what the authors called a linear correlation between saturation and brightness. Random samples were taken from natural hazy scene. Three blocks of 40×40 pixels are picked in different spot of the image: near, middle, and far (see Figs. 4). Comparing saturation and brightness (see Fig. 6) it was clearly seen that the difference and its correlation to the scene depth. The mean of the saturation and brightness was calculated. Considering that the correlation between density of the haze and the scene's depth, the result is:

$$d \propto h \propto v - s \quad (5)$$

where d, h, v and s are the depth of scene, the haze density, brightness, and saturation respectively. This statistical measure is called color attenuation prior [14].

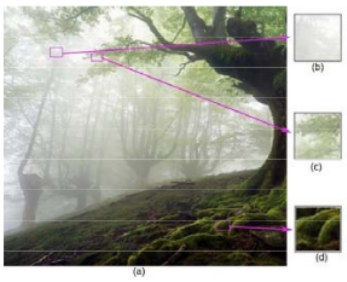

Figs. 4. The intensity of haze and scene are correlated. (a) Full scene, (b) Far scene, (c) Middle scene, and (d) Near scene

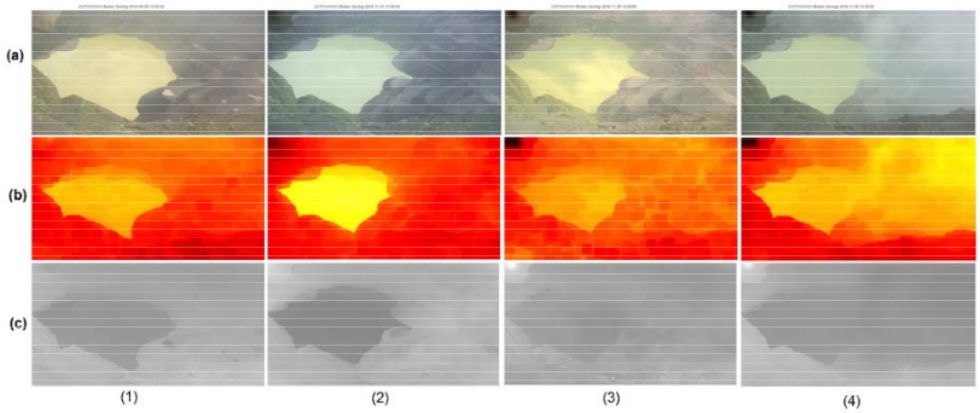

Figs. 5. Hazy image processing until transmission map using parameters gained from training. (a) Input hazy images, (b) our depth map, and (c) our refined transmission map

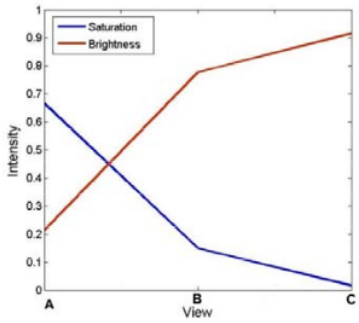

Fig. 6. Saturation starts descending for near to far view (A), (B) and (C) respectively. And vice versa for the brightness value. It starts ascending for near to far object. We get these values by taking the mean of each patches as samples

III.3. Atmospheric Light Estimation

In natural outdoor images, where the proportion of scene is adequate, human eyes can clearly distinguish between sky and land. Mostly, the sky area is the source of light. The sunlight propagates through the atmosphere. When it collides with thick clouds, light is dispersed [35], [37]. This dispersion causes clouds to be brighter. Other possibilities sources of light are object reflecting the sunlight. An object brighter than the sky can greatly affect the radiance of the scene. Since the camera position on the top of Mt. Kelud is directly facing the lake and the lake reflects the sunlight with good weather it is difficult to estimate the atm light. Moreover, the emitted fog sometimes can become the light source (see Fig. 5(b)(4)). The other light source comes from an object that reflects the light (see Figs. 5(b)(1)-(3)). This can be proved by using the DCP assumption [14], [15] by picking the brightest color or using quad-tree subdivision from [25].

Based on DCP, in a hazy scene there are some parts with high intensity. The pixels sorted in descending order according to its intensity. Then, the top 0.1 % of the brightest pixels were picked from dark channel [15], [29]. As proposed by He [15], the dark channel could be achieved by getting the lowest intensity (see Eq. (6)) color channel from certain size patches:

$$\mathbf{J}^{dr}(m) = \min_{y \in p(x)} \left(\min_{c \in \{r,g,b\}} \left(\mathbf{J}_{\mathbf{c}}(n) \right) \right) \tag{6}$$

where $\mathbf{J}^{dr}$ is the dark channel, c is the RGB channel, m is the position within video frame, and n is position within frame patches $p(m)$ positioned in m.

III.4. Depth and Transmission Map Estimation

Predicting the medium transmission in hazy scenes is an ill-posed problem. Numerous transmission map estimation approaches have been developed based on DCP [22], [26], [38]. He [15] has been using different equations for $t(m)$ which results:

$$tmap(m) = 1 - \omega \min_{y \in p(m)} \left(\min_{c} \frac{\mathbf{I}_c(n)}{\mathbf{a}_c} \right) \tag{7}$$

where $tmap$ is the medium transmission, ω is a contant valued 0.95 to keep the aerial perspective [15], $\mathbf{I}$ are input hazy frames, and $\mathbf{a}$ is atmosphere source. The problem in eq. (7) is that the result $tmap$ depends on the $\mathbf{a}$. The low value of $\mathbf{a}$ leads to darker frames and oversaturation for bright objects other than sky. Assuming that depth is limited to certain threshold, the result is:

$$d(m) = d_{thres} \tag{8}$$

where d_{thres} is the depth limit. The depth scene, $d(m)$ in Eq. (2), represents the range within the frame. Since Eq. (5) is based intuitive result, a robust model could be furtherly defined as follows:

$$d(m) = \lambda_1 + \lambda_2 v(m) + \lambda_3 s(m) \quad (9)$$

where $d(m)$ is the depth map centered at m, λ_1, λ_2 and λ_3 are coefficients respectively. Inspired by Zhu's [14] approarch, the Gaussion distribution for random error ε and zero mean variances for σ^2 were used, and the result is:

$$d(m) \sim p\left(d(m) \middle| x, \lambda_1, \lambda_2, \lambda_3\right) = N\left(0, \sigma^2\right) \quad (10)$$

$$N\left(0, \sigma^2\right) = N\left(\lambda_1 + \lambda_2 v + \lambda_3 s\right) \quad (11)$$

By using the maximum likelihood estimation for each coefficient, from Eq. (8), the result is:

$$L = \prod_{i=1}^{n} \frac{1}{\sqrt{2\pi\sigma^2}} e^{\frac{d_i - \left(\lambda_1 + \lambda_2 v(m_i) + \lambda_3 s(m_i)\right)}{2\sigma^2}} \quad (12)$$

By maximizing L it is possible to estimate the parameters $\lambda_1, \lambda_2, \lambda_3$ and σ. Both sides are taken from Eq. (11) using the natural logarithmic and partial derivative for each parameter. To assist the calculation, the matrix $\mathbf{P}$ and vector $\mathbf{r}$ were declared, then the previous matrix complemented vector $\mathbf{f}$, the result is:

$$\mathbf{P} = \begin{bmatrix} 1 & v_0 & s_0 \\ 1 & v_1 & s_1 \\ 1 & \dots & \dots \\ 1 & \dots & \dots \\ 1 & v_n & s_n \end{bmatrix}, \mathbf{r} = \begin{bmatrix} \lambda_1 \\ \lambda_2 \\ \lambda_3 \end{bmatrix}, \mathbf{f} = \begin{bmatrix} d_0 \\ d_1 \\ \dots \\ \dots \\ d_n \end{bmatrix} \quad (13)$$

By combining Eq. (12) and Eq. (13), we get:

$$\mathbf{r} = \left(\mathbf{P}^{\mathbf{T}}\mathbf{P}\right)^{-1}\mathbf{P}^{\mathbf{T}}\mathbf{f} \quad (14)$$

50 sample images sized 600 x 400 pixel were collected from Google, a total 1.2 million points for this training. Then, we get the result to restore the transmission map. The result was tested (see Figs. 5) using parameters λ_1, λ_2, and λ_3 to extract the transmission map from dark channel. The restored transmission map contains patches. In order to preserve the original quality, the result needs to be smoothed the result.

III.5. Enhanced Dehazing Scene Recovery

Since the condition on the top of summit is fluctuatively changing, the captured videos usually yield various scene colors. In prior research proposed algorithms [14], [15], they used the same technique based on the existing color channel and model in Eq (1) result in color distortion at a certain condition. However, the authors were able to reduce color distortion.

One of the key for dehazing is restoring the medium transmission. Here, a method for gamma correction was adapted. The new enhanced transmission for our method is:

$$t_{en}(m) = V_{maks}\left(\frac{tmap(m)}{V_{maks}}\right)^{\gamma} \quad (15)$$

$$\gamma = \begin{cases} 1 + \dfrac{z}{T_{thres}} & , z \geq T_{thres} \\ 1 & , z < T_{thres} \end{cases} \quad (16)$$

where $t_{en}(m)$ is the enhanced transmission map, V_{maks} is the maximum intensity from grayworld frame, γ is the adaptive gamma value obtained from Eq.(16), z is the intensity value where the cumulative distribution function (cdf) reaches 0.1, and T_{thres} is the limit intensity. The value of T_{thres} was set to 110. This value is obtained from observing data using crater lake images from clear to cloudy weather. It was found that for $z = 0.1$, the minimum T_{thres} is 110.

Inspired by [36] for recovering scene on bad weather, we calculate the mean of each pixel RGB channel. Here, the result is:

$$\mu_c = \frac{1}{s}\sum_{x=1}^{p}\sum_{y=1}^{q} G_c(x, y) \quad (17)$$

where μ_c is the average intensity of each color channel, s is the total of pixels, p, q are height and width of each frame respectively, and G_c is the intensity position (x, y). Each channel with the average intensity μ was subtracted, therefore:

$$\delta_c = \mu_x - \mu_c \quad (18)$$

where δ is the different color pixel, μ_x is average of one channel x where $x \in \{r, g, b\}$

Now, there is all needed to recover the radiance of scene **J** according to Eq. (1). Since the atm light **a** has been estimated and the enhanced transmission map t_{en} is known from Eq (14) and Eq (15), the recovered scene can be defined as:

$$\mathbf{J}_c(m) = \left(\mathbf{a}_c - \delta_c\right) + \frac{\mathbf{I}_c(m) - \mathbf{a}_c + \delta_c}{t_{en}(m)} \quad (19)$$

where $\mathbf{J}_c(m)$ is the recovered scene radiance, $\mathbf{a}$ is the estimated atm light, $\mathbf{I}$ are input hazy frames, δ is the average color difference, and $tmap(m)$ is the estimated transmission map. The proposed method managed to dehaze, as shown in Fig. 10(f).

IV. Experiments and Results

Finally, algorithms were tested with images of pumpkins and crowded people. The purpose of this test that we want to know the performance of this method compared to the previous dehazing method. The performance measured were fog density and entropy.

In this section, the performance of the proposed method was evaluated by comparing it with the previous 4 dehazing algorithms. One of them is the most popular dehazing algorithm, the DCP proposed by He [15], the second one is based on adaptive DCP [21], the third is from [39], the fourth is from [14], and the last one is from [38]. Let's call the four algorithms by He (DCP), Meng (ADCP), Tarel, Zhu (CAP), and from Chen for High-Speed Gain Intervention Refinement (HGIR).

The experiment was conducted using a PC with 2 GB RAM memory, Intel Core i5 processor, CPU clock 1.70 GHz, and NVIDIA GeForce 740M. The first step for video extraction was to load the video. Then, each frame was splitted and processed for each algorithm. This video contained 30 frames per second, RGB sized 800 x 450 pixel. The lake was recorded for about 1 minute. After frame extraction, the following step was the preparation for the dehazing procedure. The first step was taking the dark channel of each frame. From this dark channel, it was picked the top 0.1 % brightess pixel as inspired by [15], [36].

IV.1. Medium Transmission Enhancement

In this part, the proposed method was simulated using generated data obtained from Google. The method was compared with the previous dehazing methods. Guided image filtering [16] was also implemented to smooth the result because dark channel patches contain block of windows [15], [40].

When airlight was estimated, the transmission map value was separately estimated. As in Eq. (2), $tmap(m)$ depends on the depth map. The depth $d(m)$ was estimated from Eq. (9) using the pseudo-inverse matrix as in Eq. (14). The results of this training are the coefficient parameters $\lambda_1 = 0.0910$, $\lambda_2 = 0.6960$, and $\lambda_3 = -0.7198$.

The transmission map opposites its depth. The video tends to be slow. The haze moves slowly. He used Eq. (7) to estimate the transmission map. However, the resulted *tmap* may cause oversaturation (see Fig. 10(b)(1)). Chen's [38] proposed a *tmap* estimation using HGIR filter obtained from calculating the different intensities between the dark channel and minimum channel for each pixel and then dividing by the total number of pixels in the dark channel. Instead of using the assumption of *tmap* estimation, by which it is possible to get the estimated depth map, the transmission map was directly calculated using Eq. (2). The scattering coefficient β can be abandoned in case of homogeneous atmosphere.

The final task of this proposed method is the restoration of scene radiance. As we have the atm light **a** and transmission map *tmap* , prior to the final task, there is one last step that must be done. The restored image when using *tmap* without gamma correction is still not quite satisfying. The color of the ground around the lake is still influenced by, mostly, the global scene color such as blue when the haze is thicker. Therefore, the luminance of the ground could be obstructed. In order to overcome this problem, the solution is enhancing the luminance color by using popular color enhancement called gamma correction. The gamma value for normal image scene is equal to 1. Normally, for outdoor grayscale images, when the value is lower than 1, the luminance color will increase. And vice versa. In this case, the gamma correction for *tmap* was implemented. Thus, the value of gamma must be higher than 1 if the aim is to increase the luminance. The gamma value was instead limited to prevent oversaturation which may be caused by the high intensity lake color (as we can see in Figs. 10).

Different conditions of the crater lake require different handlings from gamma correction. AdaptGC was utilized rather than manually setting the gamma value. In previous research [31], before the incorporation of AdaptGC, the process of dehazing solely relied on restoring the scene radiance without enhancing the contrast. Therefore, the restored color is still influenced by the global luminance. This is one of the shortcomings of CAP compared to DCP, when the DCP can remove haze but still results in oversaturation for the lake (see Fig. 10(b)(1)).

To maintain or even to strengthen the enhanced *tmap*, we should find the mean of each pixel in the RGB channel should be found by using Eq.(15). The averaging process is capable of distributing color by enhancing it with AdaptGC. Finally, the scene was restored using Eq.(17).

IV.2. Simulation Results

In this part, the proposed method was simulated along with other algorithms Tarel [39], He *et al* for the DCP with guidance image filter [15], [16], Meng for ADCP [21], Zhu *et al* for CAP [14], Chen *et al* for HGIR based on DCP [38] for various outdoor images. A haze-free scene image must have certain requirements. Those are the consistency of color and the lowest possible content of block-like artifacts and halo effects.

Popular sample images, which have been used in many dehazing algorithms, were taken for comparison. The pumpkin image seen in Figs. 7 was compared. In

Tarel's result, it was able to restore dense fog. The distant pumpkin's contrast increased. Not many of the halo effects are shown in this data. The edge of the pumpkin tends instead to be overcontrast in white color. The DCP also can handle thick haze. The edges of the pumpkin can be preserved but the sky region may fail. It tends to be oversaturated, which results in the appearance of red color on the sky. In some parts of the pumpkins, halo effects and artifacts appeared. DCP results are almost similar to ADCP, but the oversaturation in ADCP is reduced.

In HGIR, the color of pumpkins is oversaturated and the haze is just slightly reduced. The proposed algorithms and CAP result seem similar. As shown on Fig. 7(g) (the blue arrows), the proposed method is able to increase color contrast for near objects.

The algorithm was also compared on the people crowd image, as shown in Figs. 8. The skin color of people has high contrast which results in a clear distinguished color between dark brown and light brown. For distant people, DCP gives better result than ADCP but still gives block-like artifacts. The ADCP distant object color is affected by global color. Thus, the result of ADCP tends to be bluish. Equal to the pumpkin results, HGIR also tends to be oversaturated. The skin, flower, and bandana colors are more in contrast than the others. Also, in some edges, CAP tends to be brighter. For example: the edge of the jacket corner is getting brigther. In the proposed method, the face brown color are almost evenly distributed. This makes the face color look natural.

IV.3. Quantitative Results

In order to ease the analysis, different images of crater lake were taken under any weather condition. 15 images were taken for comparison. Then, all the images were sorted by the name that preceeded by Img_ (such as, Img_1, Img_2, ... , Img_15). Our results were compared with different algorithms in terms of FADE and Entropy. The higher the FADE value the smaller the fog density vise versa. Table I shows the result of evaluation using FADE. CAP results achieved the highest FADE value compared to the others. CAP algorithm achieved the highest value of FADE. This method failed in removing thick haze. HGIR has a slightly lower average value than CAP followed by Tarel's and ADCP. The DCP has a slight average fog estimation than ADCP and also overpowered the other methods four times for Img_6, Img_8, Img_11, and Img_14. The proposed method managed to have the best fog density estimation for the average value.

As shown in Table II, entropy values from all algorithms are compared. The best value was given by CAP. Its high entropy value and low standard deviation makes the CAP the best method. Under some conditions (Img_3, Img_8, Img_9), the DCP get the top position of entropy among the others. And for once, ADCP is also capable of getting the highest entropy for Img_13. Neither Tarel nor HGIR are able to get the highest entropy. In some conditions the proposed method manages to get the highest entropy value but the average value was the second lowest after Tarel's. This was mainly caused by high entropy variance values. Overall, if we sort the algorithms for entropy, the rank shows that Tarel is the last. And the top is CAP. This achievement is caused by the capability of CAP of preserving detail while the second is DCP for all 15 images. As shown in Table I, the proposed method gave the best results compared to the other algorithms in terms of fog density (1.60912). However, it achieved small values based on entropy, compared to the others. Zhu achieved best entropy value (7.352013). In Figs. 10, the image restored using the proposed method is shown with different gamma values.

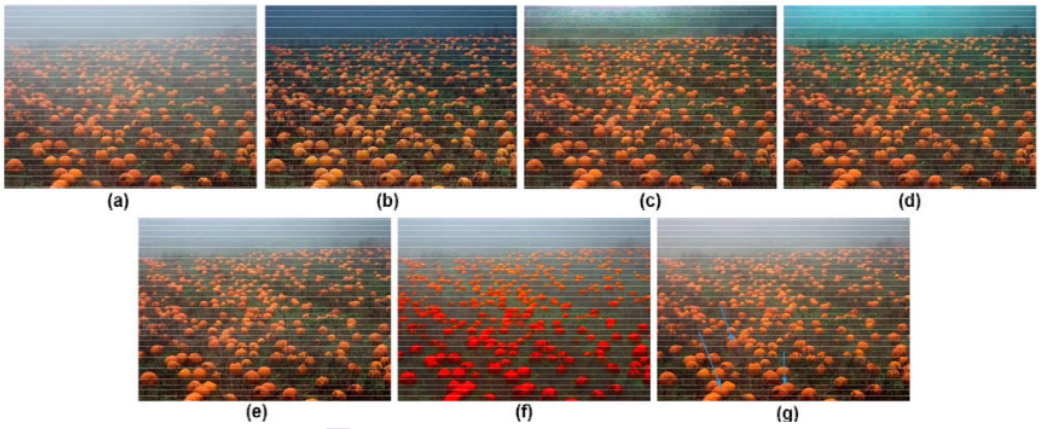

Figs. 7. Simulation result using pumpkins image. (a) Input hazy image, (b) Tarel, (c) DCP, (d) ADCP, (e) CAP, (f) HGIR, and (g) Our result

Figs. 8. Simulation result using people image. (a) Input hazy image, (b) Tarel, (c) DCP, (d) ADCP, (e) CAP, (f) HGIR, and (g) Our result. The edge and overcontrast of image can be seen clearly

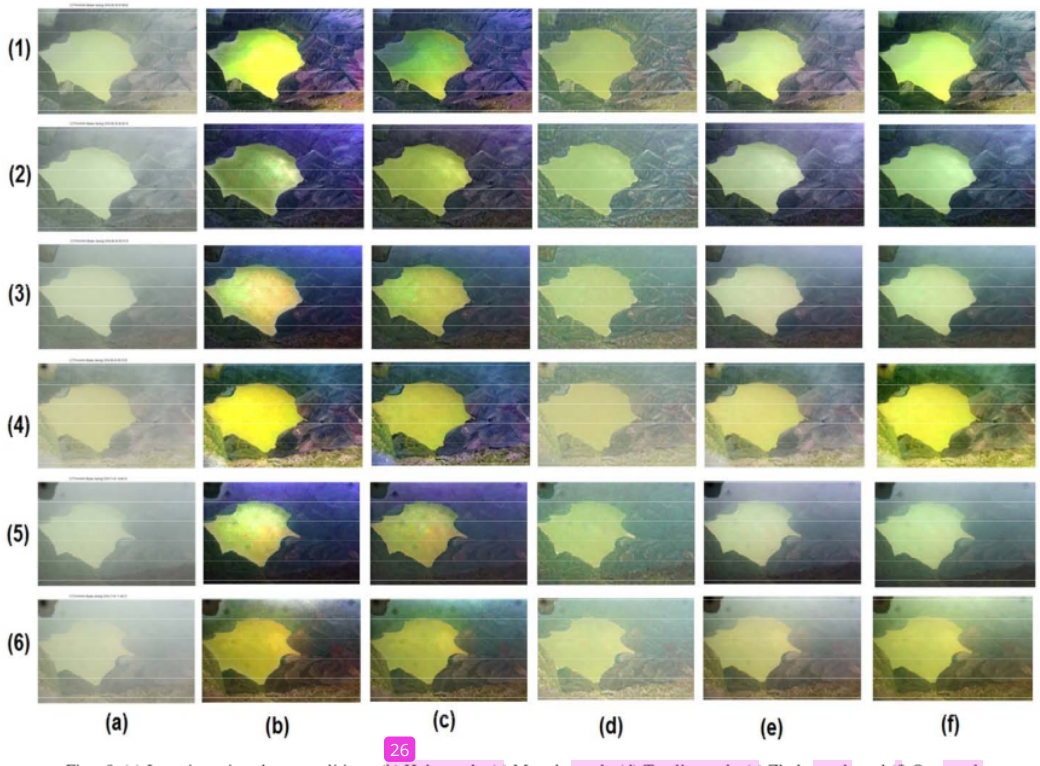

Figs. 9. (a) Input in various hazy conditions. (b) He's result, (c) Meng's result, (d) Tarel's result, (e) Zhu's result, and (f) Our result

TABLE I
FADE DATA

Image name	Algorithms					
	Tarel	DCP	ADCP	CAP	HGIR	Our
Img_1	1.9779	1.5885	1.6848	2.2714	2.1634	**1.1653**
Img_2	2.6072	1.7083	1.9582	2.268	2.1385	**0.9886**
Img_3	3.0589	1.7016	1.7284	2.5594	2.2876	**1.2604**
Img_4	2.558	1.9048	2.3111	2.6533	2.1942	**1.3162**
Img_5	2.8491	1.9587	2.1463	2.9275	2.5315	**1.8896**
Img_6	2.558	**2.1698**	2.2606	3.261	3.0208	2.4518
Img_7	2.3874	1.8043	1.9899	2.6297	2.4353	**1.7896**
Img_8	2.3414	**2.0317**	2.4234	3.2869	2.9615	2.3768
Img_9	2.4587	1.7608	1.8332	2.4332	2.5266	**1.2229**
Img_10	2.3167	1.7709	2.0675	2.5813	2.3195	**1.6619**
Img_11	2.8187	**1.7327**	1.9634	2.7007	2.6183	2.0876
Img_12	2.3836	1.9021	2.1823	2.5032	2.6523	**1.2936**
Img_13	2.4378	1.6172	1.7776	2.4833	2.2876	**1.5567**
Img_14	2.3621	**1.9062**	2.1475	2.8291	2.6004	1.9936
Img_15	2.3983	2.0098	2.44	2.9422	2.9911	**1.0822**
Avg	2.50092	1.837827	2.060947	2.68868	2.51524	**1.60912**

TABLE II
ENTROPY DATA

Image name	Algorithms					
	Tarel	DCP	ADCP	CAP	HGIR	Our
Img_1	7.0898	7.4764	7.4439	**7.6687**	7.3795	6.9533
Img_2	6.7091	6.9826	6.8403	**7.2583**	6.7122	4.1988
Img_3	6.376	**7.4821**	7.2956	7.0659	7.2437	7.3422
Img_4	6.8837	6.8617	6.7322	**7.4558**	7.2307	6.9232
Img_5	6.6446	7.218	6.9856	7.2073	7.3039	**7.609**
Img_6	6.8595	7.4033	7.1082	7.2812	7.3588	**7.5075**
Img_7	6.864	7.1345	7.0662	7.4287	7.4019	**7.4701**
Img_8	7.2338	**7.4828**	7.1507	7.2862	7.3454	7.4796
Img_9	6.9434	**7.3185**	7.2106	7.33	7.0981	6.8937
Img_10	6.8551	7.2254	6.9903	7.466	7.5145	**7.5315**
Img_11	6.67	7.4014	7.0411	7.1579	7.2585	**7.4622**
Img_12	7.0271	7.3139	7.0806	**7.6632**	7.3768	6.784
Img_13	6.9425	7.0882	**7.3142**	7.1567	6.8411	7.1569
Img_14	6.9228	7.5293	7.1168	7.4646	7.5493	**7.5974**
Img_15	7.052	7.1915	6.8821	**7.3897**	7.2721	5.3001
Avg	6.87156	7.273973	7.083893	**7.352013**	7.2591	6.9473

IV.4. Qualitative Results

Almost every haze removal algorithms is capable of getting good results by removing haze in outdoor images. However, it is hard to measure them just by viewing. Thus, the previous algorithms were compared under different weather conditions with various haze densities. Some of the images contained bright objects which make most of dehazing algorithms prone to overbrightness.

The previous state-of-the-art dehazing algorithms [14], [15], [21], [39] are compared on crater lake images. Fig. 9(a) is the original input hazy image, Fig. 9(b) to Fig. 9(e) are the results of He et al, Meng et al, Tarel et al, and Zhu et al. And finally Fig. 9(f) is the proposed dehazing method.

Fig. 7(b) and Fig. 7(d) show an almost perfect ability to remove haze which belongs to He's and Tarel's respectively. He's result tend to oversaturate because the lake color is brighter than other objects. When the haze getting thicker, Meng's and He's result tend to be bluish for the land around the lake because of the dominant blue-greenish color. The crater lake images were tested using DCP algorithms. The halo effect appeared around the edge of lake as we can see clearly on Fig. 9(2)(b), Fig. 9(3)(b), and Fig. 9(6)(b). This happened mainly due to the block artifacts from dark channel itself. This halo effect can be reduced by using ADCP. A small amount of shadows, probably from the cloud which passed through above the lake appeared as a reflection on the surface of

the lake water. Both DCP and ADCP leave the dense haze effect above the area of the image (see Fig. 9(6)(b) and Fig. 9(6)(c).

Meng *et al.*'s results are almost similar to the result of He *et al*. Since Meng *et al* method advances the DCP technique using the boundary constraint. Our results compared to Zhu et al.'s results are closely equal. This happened due to the fact that the proposed method was developed based on color attenuation prior enhanced color strenching by reducing atmospheric light by average color channel.

In Tarel's, the edge of object such as truck trails and rocks can be clearly seen in Figs. 9(1)(d) – (6)(d). But, Tarel's could not handle thick fog. Moreover, Tarel's algorithm could not remove the fog in small edge regions. The haze still remains in some corners of the lake, as shown on Fig. 9(1)(d), Fig. 9(2)(d), Fig. 9(3)(d), and Fig. 9(5)(d). The upper limit and lower limit for the corrected gamma were taken as 2.75 and 1, respectively. The traditional gamma correction identifies that the higher gamma value means a darker image. And the lower gamma value will cause images to be brighter. Normally, the gamma is used to correct a grayscale image. But, in our case, since we corrected only the transmission map, the higher corrected gamma value results in oversaturation on the lake and the land around it will be darker.

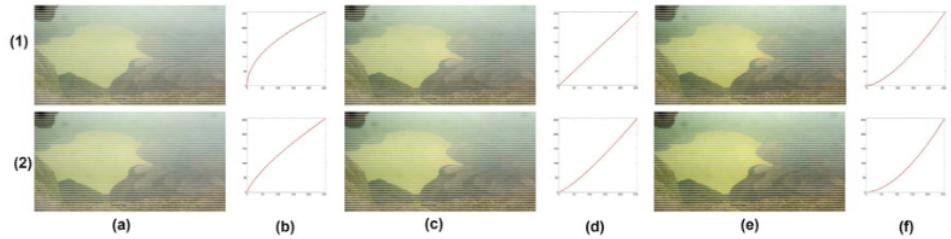

Figs. 10. Various restored images with its corresponding gamma value. (1b) γ = 0.5, (2b) γ = 0.75, (1d) γ = 1.0, (2d) γ = 1.25, (1f) γ = 1.50, and (2f) γ = 1.75

V. Conclusion and Discussion

In this paper, a dehazing technique was proposed based on color attenuation prior and adaptive limited gamma correction. This approach incorporates state-of-the-art methods: dark channel prior, color attenuation prior, and gamma correction.

The proposed method gains the second lowest result in entropy (6.9473) and the best fog density estimation (1.60912). With enhanced color using adaptive gamma correction, this method achieved superiority over previous approaches yet still it is not possible to recover the true lake color since the dominance environment color affects the results. Interestingly, this problem proves that dehazing is an ill-posed problem.

In natural images, some scenes contain both foreground and background objects. Our method failed to preserve the color of foreground object. This will be the focus of future research on the dehazing process, separating foreground and background objects so that the color of foreground objects can be preserved.

Acknowledgements

The authors would like to thank the Indonesia Endowment Fund or Lembaga Pengelola Dana Pendidikan (LPDP) for this work as sponsorship and Pusat Vulkanologi dan Mitigasi Bencana Geologi Gunung Kelud for providing data and helping the analysis.

References

[1] I. Pratomo, "Klasifikasi Gunung Api Aktif Indonesia , Studi Kasus dari Beberapa Letusan Gunung Api dalam Sejarah," *J. Geol. Indones. Vol. 1 No. 4 Desember 2006*, vol. 1, no. 4, pp. 219–227, 2006.

[2] Y. Nakashima, K. Heki, A. Takeo, M. N. Cahyadi, A. Aditiya, and K. Yoshizawa, "Atmospheric resonant oscillations by the 2014 eruption of the Kelud volcano, Indonesia, observed with the ionospheric total electron contents and seismic signals," *Earth Planet. Sci. Lett.*, vol. 434, pp. 112–116, 2016.

[3] S. Andreastuti, E. Paripurno, H. Gunawan, A. Budianto, and D. Syahbana, "Character of community response to volcanic crises at Sinabung and Kelud volcanoes," *J. Volcanol. Geotherm. Res.*, 2017.

[4] A. Jolly, B. Kennedy, M. Edwards, P. Jousset, and B. Scheu, "Infrasound tremor from bubble burst eruptions in the viscous shallow crater lake of White Island, New Zealand, and its implications for interpreting volcanic source processes," *J. Volcanol. Geotherm. Res.*, vol. 327, pp. 585–603, 2016.

[5] P. Bani, G. Boudon, H. Balcone-Boissard, P. Delmelle, T. Quiniou, J. Lefevre, E. G. Bule, S. Hiroshi, and M. Lardy, "The 2009-2010 eruption of Gaua volcano (Vanuatu archipelago): Eruptive dynamics and unsuspected strong halogens source," *J. Volcanol. Geotherm. Res.*, vol. 322, pp. 63–75, 2016.

[6] C. Hom, P. Metzler, K. Ullrich, M. Koschorreck, and B. Boehrer, "Science of the Total Environment Methane storage and ebullition in monimolimnetic waters of polluted mine pit lake Vollert-Sued , Germany," *Sci. Total Environ.*, vol. 584–585, pp. 1–10, 2017.

[7] P. Allard, M. Burton, G. Sawyer, and P. Bani, "Degassing dynamics of basaltic lava lake at a top-ranking volatile emitter: Ambrym volcano, Vanuatu arc," *Earth Planet. Sci. Lett.*, vol. 448, pp. 69–80, 2016.

[8] X. Xi, M. S. Johnson, S. Jeong, M. Fladeland, D. Pieri, J. A. Diaz, and G. L. Bland, "Constraining the sulfur dioxide degassing flux from Turrialba volcano, Costa Rica using unmanned aerial system measurements," *J. Volcanol. Geotherm. Res.*, vol. 325, pp. 110–

[9] C. Caudron, R. Campion, D. Rouwet, T. Lecocq, B. Capaccioni, D. Syahbana, Suparjan, B. H. Purwanto, and A. Bernard, "Stratification at the Earth's largest hyperacidic lake and its consequences," *Earth Planet. Sci. Lett.*, vol. 459, pp. 28–35, 2017.

[10] C. S. Hayer, G. Wadge, M. Edmonds, and T. Christopher, "Sensitivity of OMI SO2 measurements to variable eruptive behaviour at Soufrière Hills Volcano, Montserrat," *J. Volcanol. Geotherm. Res.*, vol. 312, pp. 1–10, 2016.

[11] K. Eka, P. Sofyan, S. Pretina, and S. B. Ugan, "Karakteristik kimiawi air danau kawah Gunung Api Kelud , Jawa Timur pasca letusan tahun 1990," *Indones. J. Geosci.*, vol. 1, no. 4, pp. 185–192, 2006.

[12] M. Gresse, J. Vandemeulebrouck, S. Byrdina, G. Chiodini, and P. P. Bruno, "Changes in CO2 diffuse degassing induced by the passing of seismic waves," *J. Volcanol. Geotherm. Res.*, vol. 320, pp. 12–18, 2016.

[13] R. W. Henley and G. O. Hughes, "SO2 flux and the thermal power of volcanic eruptions," *J. Volcanol. Geotherm. Res.*, vol. 324, pp. 190–199, 2016.

[14] Q. Zhu, J. Mai, L. Shao, and S. Member, "A Fast Single Image Haze Removal Algorithm Using Color Attenuation Prior," *IEEE Trans. Image Process.*, vol. 24, no. 11, pp. 3522–3533, 2015.

[15] K. He, J. Sun, and X. Tang, "Single image haze removal using dark channel prior," *IEEE Trans. Pattern Anal. Mach. Intell.*, vol. 33, no. 12, pp. 2341–2353, 2011.

[16] K. He, J. Sun, and X. Tang, "Guided Image Filtering," *IEEE Trans. Pattern Anal. Mach. Intell.*, vol. 35, no. 6, pp. 1397–1409, 2013.

[17] Z. Huang, T. Zhang, Q. Li, and H. Fang, "Adaptive gamma correction based on cumulative histogram for enhancing near-infrared images," *Infrared Phys. Technol.*, vol. 79, pp. 205–215, 2016.

[18] L. K. Choi, J. You, and A. C. Bovik, "Referenceless Prediction of Perceptual Fog Density and Perceptual Image Defogging," *IEEE Trans. Image Process.*, vol. 24, no. 11, pp. 3888–3901, 2015.

[19] R. Fattal, "Single Image Dehazing," *ACM Trans. Graph.*, vol. 27, no. 3, p. 72:1--72:9, Aug. 2008.

[20] R. T. Tan, "Visibility in Bad Weather from a Single Image," 2008.

[21] G. Meng, Y. Wang, J. Duan, S. Xiang, and C. Pan, "Efficient Image Dehazing with Boundary Constraint and Contextual Regularization," in *2013 IEEE International Conference on Computer Vision*, 2013, pp. 617–624.

[22] M. Yang, Z. Li, and J. Liu, "Super-pixel Based Single Image Haze Removal," in *2016 Chinese Control and Decision Conference (CCDC)*, 2016, pp. 1965–1969.

[23] B. Cai, X. Xu, K. Jia, C. Qing, and D. Tao, "DehazeNet: An End-to-End System for Single Image," *IEEE Trans. Image Process.*, vol. 25, no. 11, pp. 5187–5198, 2016.

[24] A. Galdran, J. Vazquez-corral, D. Pardo, and M. Bertalm, "Fusion-Based Variational Image Dehazing," *IEEE Signal Process. Lett.*, vol. 24, no. 2, pp. 151–155, 2017.

[25] J. H. Kim, W. D. Jang, J. Y. Sim, and C. S. Kim, "Optimized contrast enhancement for real-time image and video dehazing," *J. Vis. Commun. Image Represent.*, vol. 24, no. 3, pp. 410–425, 2013.

[26] L. Zeng and Y. Dai, "Single Image Dehazing Based on Combining Dark Channel Prior and Scene Radiance Constraint," *Chinese J. Electron.*, vol. 25, no. 6, pp. 1114–1120, 2016.

[27] Q. Zhang, Y. Nie, L. Zhang, and C. Xiao, "Underexposed Video Enhancement via Perception-Driven Progressive Fusion," *IEEE Trans. Vis. Comput. Graph.*, vol. 22, no. 6, pp. 1773–1785, 2016.

[28] Pujiono, P., Yuniarno, E., Purnama, I., Andono, P., Hariadi, M., Underwater Coral Reef Color Image Enhancement Based on Polynomial Equation, (2016) *International Review on Computers and Software (IRECOS)*, 11 (2), pp. 143-150.

[29] C. Y. Li, J. C. Guo, R. M. Cong, Y. W. Pang, and B. Wang, "Underwater image enhancement by Dehazing with minimum information loss and histogram distribution prior," *IEEE Trans. Image Process.*, vol. 25, no. 12, pp. 5664–5677, 2016.

[30] B. Gupta and M. Tiwari, "Minimum mean brightness error contrast enhancement of color images using adaptive gamma correction with color preserving framework," *Optik (Stuttg).*, vol. 11, no. 4, pp. 1671–1676, 2016.

[31] O. V Putra, B. Prianto, E. M. Yuniarno, and M. H. Purnomo, "Visibility restoration of lake crater hazy image based on dark channel prior," in *2016 International Computer Science and Engineering Conference (ICSEC)*, 2016, pp. 1–6.

[32] C. Jung, Q. Yang, T. Sun, Q. Fu, and H. Song, "Low Light Image Enhancement with Dual-Tree Complex Wavelet Transform," *J. Vis. Commun. Image Represent.*, vol. 42, pp. 28–36, 2016.

[33] A. Kaur and C. Singh, "Contrast enhancement for cephalometric images using wavelet-based modified adaptive histogram equalization," *Appl. Soft Comput.*, vol. 51, pp. 180–191, 2017.

[34] S. G. Narasimhan and S. K. Nayar, "Chromatic framework for vision in bad weather," in *Computer Vision and Pattern Recognition, 2000. Proceedings. IEEE Conference on*, 2000, vol. 1, pp. 598–605 vol.1.

[35] S. G. Narasimhan and S. K. Nayar, "Vision and the Atmosphere," *Int. J. Comput. Vis.*, vol. 48, no. 3, pp. 233–254, 2002.

[36] S. C. Huang, B. H. Chen, and W. J. Wang, "Visibility restoration of single hazy images captured in real-world weather conditions," *IEEE Trans. Circuits Syst. Video Technol.*, vol. 24, no. 10, pp. 1814–1824, 2014.

[37] C. McHardy, T. Horneber, and C. Rauh, "Spectral simulation of light propagation in participating media by using a lattice Boltzmann method for photons," *Appl. Math. Comput.*, vol. 0, pp. 1–12, 2017.

[38] B. H. Chen, S. C. Huang, and F. C. Cheng, "A high-efficiency and high-speed gain intervention refinement filter for haze removal," *J. Disp. Technol.*, vol. 12, no. 7, pp. 753–759, 2016.

[39] J.-P. Tarel and N. Hauti, "Fast Visibility Restoration from a Single Color or Gray Level Image," in *2009 IEEE 12th International Conference on Computer Vision (ICCV)*, 2009, no. August 2015.

[40] N. Baig, M. M. Riaz, A. Ghafoor, and A. M. Siddiqui, "Image Dehazing Using Quadtree Decomposition and Entropy-Based Contextual Regularization," *IEEE Signal Process. Lett.*, vol. 23, no. 6, pp. 853–857, 2016.

Authors' information

[1]Department of Electrical Engineering, Institut Teknologi Sepuluh Nopember, Surabaya, Indonesia.
[2]Department of Informatics, Universitas Darussalam Gontor, Ponorogo, Indonesia.
[3]Center of Volcanology and Geological Disaster Mitigation, Ministry of Energy and Mineral Resources, Bandung, Indonesia
[4]Department of Information Technology, Universitas Widya Kartika, Surabaya, Indonesia.
[5]Department of Information Technology, Sekolah Tinggi Teknik Surabaya, Surabaya, Indonesia..

Oddy Virgantara Putra was born on August, 24th 1988. He received his B.S. in computer at the Department of Information System in Institut Teknologi Sepuluh Nopember (ITS), Surabaya, Indonesia in 2012. He is currently student of Department of Electrical Engineering for master field in intelligence network multimedia. His current research interests are computer vision, image processing, and data mining.

Budi Prianto was born on December 1st, 1970. He graduated from vocational senior highschool UZIEL in Kediri, Indonesia in 1991. He currently is a researcher in Center of Vulcanology and Mitigation Geological Disaster (Pusat Vulkanologi dan Mitigasi Bencana Geologi) in March 1993. He was positioned as observer of volcano (Pusat Gunung Api) at Mt. Dieng, Central Java from 1993 until March, 2002. Starting from March 2002, he was relocated to observer of volcano (Pengamatan Gunung Api) again for Mt. Kelud.

Agus Prayitno was born on May, 14th 1975. He received his B.S. on Sekolah Tinggi Teknologi Cahaya Surya Kediri in 1996. In 2014, he received his master's degree in Telematics in Department of Electrical Engineering, Institut Teknologi Sepuluh Nopember (ITS), Surabaya, Indonesia. He is currently the head of Information Communications Technology (ICT) of the Department of Information Technology, Universitas Widya Kartika, Surabaya, Indonesia. His current research interests are computer vision, artificial intelligence, biomedical, and image processing.

Esther Irawati Setiawan received her bachelor's degree in computer science and master's degree in information technology from Sekolah Tinggi Teknik Surabaya (STTS), Surabaya, Indonesia, in 2006 and 2010 respectively. She is currently taking a Ph.D degree at Institut Teknologi Sepuluh Nopember (ITS), Surabaya, Indonesia. She joined the faculty member in STTS since 2006. Her current research interests include Machine Learning, Image Processing, Text Mining, Social Network Analysis, and Natural Language Processing.

Eko Mulyanto Yuniarno was born on June 1st, 1968. He received his B.E degree in computer system in 1995, master's degree in power system in 2005 and Ph.D degree in computer science in 2013 in Department of Electrical Engineering, Institut Teknologi Sepuluh Nopember (ITS), Surabaya, Indonesia. He currently is head of Computer Vision Laboratory in Department of Computer Engineering, Faculty of Electrical Engineering, Institut Teknologi Sepuluh Nopember (ITS), Surabaya. His research interest are computer vision, 3D reconstruction, image processing.

Mauridhi Hery Purnomo was born on September 16th, 1958. He received his B.E degree from Department of Electrical Engineering, Institut Teknologi Sepuluh Nopember (ITS), Surabaya, Indonesia in 1984. 1989, he received his master's degree from in 1989 and his Ph.D in 1995 from Osaka City University. He received his professor in artificial intelligence in 2004. He currently is the head of computer and telematics laboratory, Department of Computer Engineering, Faculty of Electrical Engineering, Institut Teknologi Sepuluh Nopember (ITS), Surabaya, Indonesia. His research interest are artificial intelligence, machine learning, data mining, and image processing.

A Novel Approach on Dehazing Volcanic Crater Lake Hazy Scene Videos Based on Color Attenuation Prior

ORIGINALITY REPORT

25%	21%	22%	12%
SIMILARITY INDEX	INTERNET SOURCES	PUBLICATIONS	STUDENT PAPERS

PRIMARY SOURCES

1	repository.its.ac.id Internet Source	8%
2	Submitted to Universiti Teknikal Malaysia Melaka Student Paper	2%
3	www.scilit.net Internet Source	2%
4	repository.uin-malang.ac.id Internet Source	1%
5	O V Putra, A Musthafa, F R Pradhana. "A Hybrid Approach on Single Image Dehazing using Adaptive Gamma Correction", Journal of Physics: Conference Series, 2019 Publication	1%
6	www.iaeng.org Internet Source	1%
7	Oddy Virgantara Putra, Budi Prianto, Eko Mulyanto Yuniarno, Mauridhi Hery Purnomo. "Visibility restoration of lake crater hazy	1%

image based on dark channel prior", 2016 International Computer Science and Engineering Conference (ICSEC), 2016
Publication

8	Submitted to Universitas Dian Nuswantoro Student Paper	1 %
9	Guojia Hou, Jingming Li, Guodong Wang, Huan Yang, Baoxiang Huang, Zhenkuan Pan. "A novel dark channel prior guided variational framework for underwater image restoration", Journal of Visual Communication and Image Representation, 2020 Publication	<1 %
10	Submitted to The University of Manchester Student Paper	<1 %
11	ejurnal.stmik-budidarma.ac.id Internet Source	<1 %
12	Alina Majeed Chaudhry, Muhammad Mohsin Riaz, Abdul Ghafoor. "A Framework for Outdoor RGB Image Enhancement and Dehazing", IEEE Geoscience and Remote Sensing Letters, 2018 Publication	<1 %
13	ejournal.unida.gontor.ac.id Internet Source	<1 %
14	www.ijitee.org Internet Source	<1 %

15	link.springer.com Internet Source	<1%
16	Hanung Adi Nugroho, Rizki Nurfauzi, Eka Legya Frannita. "Plasmodium Candidate Detection on Thin Blood Smear Images with Luminance Noise Reduction", 2019 5th International Conference on Science in Information Technology (ICSITech), 2019 Publication	<1%
17	Magudeeswaran Veluchamy, Ashish Kumar Bhandari, Bharath Subramani. "Optimized Bezier Curve Based Intensity Mapping Scheme for Low Light Image Enhancement", IEEE Transactions on Emerging Topics in Computational Intelligence, 2021 Publication	<1%
18	Junpeng Hu, Zuoyong Li, Xinwei Chen. "Modified Image Haze Removal Algorithm Based on Dark Channel Prior", 2019 IEEE Intl Conf on Parallel & Distributed Processing with Applications, Big Data & Cloud Computing, Sustainable Computing & Communications, Social Computing & Networking (ISPA/BDCloud/SocialCom/SustainCom), 2019 Publication	<1%
19	repository.unair.ac.id Internet Source	<1%

20	www.porikli.com Internet Source	<1 %
21	Pujiono Pujiono, Eko Mulyanto Yuniarno, I. Ketut Eddy Purnama, Pulung Nurtantio Andono, Mochamad Hariadi. "Underwater Coral Reef Color Image Enhancement Based on Polynomial Equation", International Review on Computers and Software (IRECOS), 2016 Publication	<1 %
22	Yun Liu, Hejian Li, Minghui Wang. "Single Image Dehazing via Large Sky Region Segmentation and Multiscale Opening Dark Channel Model", IEEE Access, 2017 Publication	<1 %
23	caibolun.github.io Internet Source	<1 %
24	ieeexplore.ieee.org Internet Source	<1 %
25	"How to Use This Book", Diffusion-Weighted MR Imaging of the Brain, 2005 Publication	<1 %
26	Submitted to Kolej MARA Seremban Student Paper	<1 %
27	Chenggang Dai, Mingxing Lin, Xiaojian Wu, Dong Zhang. "Single hazy image restoration	<1 %

	using robust atmospheric scattering model", Signal Processing, 2020 Publication	
28	Submitted to Udayana University Student Paper	<1 %
29	api.uinjkt.ac.id Internet Source	<1 %
30	ijeei.org Internet Source	<1 %
31	wrap.warwick.ac.uk Internet Source	<1 %
32	Zhengguo Li, Jinghong Zheng. "Edge-Preserving Decomposition-Based Single Image Haze Removal", IEEE Transactions on Image Processing, 2015 Publication	<1 %
33	iaescore.com Internet Source	<1 %
34	ijsret.com Internet Source	<1 %
35	paper.ijcsns.org Internet Source	<1 %
36	www.accu.or.jp Internet Source	<1 %

37	Adrian Galdran, Javier Vazquez-Corral, David Pardo, Marcelo Bertalmio. "Fusion-based Variational Image Dehazing", IEEE Signal Processing Letters, 2016 Publication	<1 %
38	Min Han, Zhiyu Lyu, Tie Qiu, Meiling Xu. "A Review on Intelligence Dehazing and Color Restoration for Underwater Images", IEEE Transactions on Systems, Man, and Cybernetics: Systems, 2019 Publication	<1 %
39	Victor H. Diaz-Ramirez, José Enrique Hernández-Beltrán, Rigoberto Juarez-Salazar. "Real-time haze removal in monocular images using locally adaptive processing", Journal of Real-Time Image Processing, 2017 Publication	<1 %
40	Yin Gao, Yijing Su, Qiming Li, Jun Li. "Single fog image restoration with multi-focus image fusion", Journal of Visual Communication and Image Representation, 2018 Publication	<1 %
41	techscience.com Internet Source	<1 %
42	Chuanzi He, Chendi Zhang, Qingrong Cheng, Xixiaoyi Jin, Jianjun Yin. "A haze density aware adaptive perceptual single image haze	<1 %

removal algorithm", 2016 IEEE International Conference on Information and Automation (ICIA), 2016
Publication

---

43 Jose Enrique Hernandez-Beltran, Victor H. Diaz-Ramirez, Leonardo Trujillo, Pierrick Legrand. "Design of estimators for restoration of images degraded by haze using genetic programming", Swarm and Evolutionary Computation, 2019
Publication

<1 %

---

44 www.hindawi.com
Internet Source

<1 %

---

45 Codruta O. Ancuti, Cosmin Ancuti, Christophe De Vleeschouwer, Laszlo Neumann, Rafael Garcia. "Color transfer for underwater dehazing and depth estimation", 2017 IEEE International Conference on Image Processing (ICIP), 2017
Publication

<1 %

---

46 Jianlei Liu. "Visibility distance estimation in foggy situations and single image dehazing based on transmission computation model", IET Image Processing, 2018
Publication

<1 %

---

47 Margo Pujiantara, Dimas Okky Anggriawan, Anang Tjahjono, Defin Permadi, Ardyono Priyadi, Mauridhi Hery Purnomo. "A Real-Time

<1 %

	Current Harmonic Monitoring System Based on Stockwell Transform Method", International Review of Electrical Engineering (IREE), 2016 Publication	
48	Shi, Zhenwei, Jiao Long, Wei Tang, and Changshui Zhang. "Single image dehazing in inhomogeneous atmosphere", Optik - International Journal for Light and Electron Optics, 2014. Publication	<1 %
49	Wei Liu, Ping Ye, Hanxu Sun. "Image Dehazing based on region growing", 2017 4th International Conference on Systems and Informatics (ICSAI), 2017 Publication	<1 %
50	Wencheng Wang, Xiaohui Yuan, Xiaojin Wu, Yunlong Liu. "Fast Image Dehazing Method Based on Linear Transformation", IEEE Transactions on Multimedia, 2017 Publication	<1 %
51	ijoer.com Internet Source	<1 %
52	nrl.northumbria.ac.uk Internet Source	<1 %
53	www.inass.org Internet Source	<1 %

54	www.intechopen.com Internet Source	<1%
55	www.ri.cmu.edu Internet Source	<1%
56	"Computer Vision – ACCV 2016 Workshops", Springer Science and Business Media LLC, 2017 Publication	<1%
57	"iCAST 2017 proceedings", 2017 IEEE 8th International Conference on Awareness Science and Technology (iCAST), 2017 Publication	<1%
58	Chu, Xiumin, YiRong Wu, Xianqiao Chen, Jingwen Lv, and Wei Liu. "Haze Removal for a Single Inland Waterway Image using Sky Segmentation and Dark Channel Prior", IET Image Processing, 2016. Publication	<1%
59	Edi Noersasongko, Guruh Fajar Shidik, Adhitya Nugraha, Pulung Nurtantio Andono, Edi Jaya Kusuma. "Automatic Integration of Ubiquitous Access Address in Camera Surveillance System Using Natural Language Processing", International Review on Modelling and Simulations (IREMOS), 2021 Publication	<1%

60	Liu, Yun-Fu, Jing-Ming Guo, and Bo-Syun Lai. "Parametric-Oriented Fitting for Local Contrast Enhancement", Information Sciences, 2016. Publication	<1 %
61	Liyun Zhuang, Yingshuang Ma, Yuanyang Zou, Guoxin Wang. "A Novel Image Dehazing Algorithm via Adaptive Gamma-Correction and Modified AMEF", IEEE Access, 2020 Publication	<1 %
62	Tiwari, Mayank, Subir Singh Lamba, and Bhupendra Gupta. "An approach for visibility improvement of dark color images using adaptive gamma correction and DCT-SVD", First International Workshop on Pattern Recognition, 2016. Publication	<1 %
63	Weijiang Wang, Yeping Peng, Guangzhong Cao, Xiaoqin Guo, Ngaiming Kwok. "Low-illumination Image Enhancement for Night-time UAV Pedestrian Detection", IEEE Transactions on Industrial Informatics, 2020 Publication	<1 %
64	Zhong Luan, Hao Zeng, Yuanyuan Shang, Zhuhong Shao, Hui Ding. "Fast Video Dehazing Using Per-Pixel Minimum Adjustment", 'Hindawi Limited', 2018 Internet Source	<1 %

65	hub.lib.ucy.ac.cy Internet Source	<1%
66	pure.ulster.ac.uk Internet Source	<1%
67	www.mdpi.com Internet Source	<1%
68	www.tandfonline.com Internet Source	<1%
69	Yongmin Park, Tae-Hwan Kim. "Fast Execution Schemes for Dark-Channel-Prior-Based Outdoor Video Dehazing", IEEE Access, 2018 Publication	<1%
70	"Advances in Multimedia Information Processing - PCM 2016", Springer Science and Business Media LLC, 2016 Publication	<1%
71	Agus Zainal Arifin, Rarasmaya Indraswari, Nanik Suciati, Eha Renwi Astuti, Dini Adni Navastara. "Region Merging Strategy Using Statistical Analysis for Interactive Image Segmentation on Dental Panoramic Radiographs", International Review on Computers and Software (IRECOS), 2017 Publication	<1%

Exclude quotes	Off	Exclude matches	Off
Exclude bibliography	Off		